DMSP SSM/I-SSMIS Daily Polar Gridded Brightness Temperatures, Version 6

USER GUIDE

How to Cite These Data

As a condition of using these data, you must include a citation:

Meier, W. N., J. S. Stewart, H. Wilcox, D. J. Scott, and M. A. Hardman. 2022. *DMSP SSM/I-SSMIS Daily Polar Gridded Brightness Temperatures, Version 6*. [Indicate subset used]. Boulder, Colorado USA. NASA National Snow and Ice Data Center Distributed Active Archive Center. https://doi.org/10.5067/MXJL42WSXTS1. [Date Accessed].

FOR QUESTIONS ABOUT THESE DATA, CONTACT NSIDC@NSIDC.ORG

FOR CURRENT INFORMATION, VISIT https://nsidc.org/data/NSIDC-0001

National Snow and Ice Data Center

TABLE OF CONTENTS

1 DATA DESCRIPTION

1.1 Parameters

The geophysical parameter of this data set is Brightness Temperature (T_b or Tb), measured in kelvins (K). Values typically range from 50.0 K to 350.0 K.

1.2 File Information

1.2.1 Format

The data are in NetCDF (.nc) format, using CF 1.6 (Climate and Forecast) and ACDD 1.3 (Attribute Conventions for Dataset Discovery) metadata conventions. In order to reduce file size without loss of data precision, the brightness temperature (Tb) values are multiplied by 10 prior and converted to two-byte integers. For example, a stored integer value of 2358 represents a brightness temperature value of 235.8 K. A value of 0 indicates missing data.

1.2.2 File Contents

The NetCDF (.nc) files come with a granule-specific metadata file, called an Extensible Markup Language (.xml) file.

The NetCDF files contain data grouped by sensor (F08, F11, F13, F17, or F18). If there are data from more than one sensor on a day, each sensor will have its own Data Group. For an example of data parameters for an F08, F11, or F13 sensor data group, see Table 1 and Table 2. For an example of data parameters for an F17 or F18 sensor group, see Table 1 and Table 3.

Table 1. Field contents for Data Group “F08” for low frequency channels with 25 km resolution.

Parameter	Description
TB_F08_19H	Brightness temperature in K for the horizontally polarized 19.3 GHz channel.
TB_F08_19V	Brightness temperature in K for the vertically polarized 19.3 GHz channel.
TB_F08_22V	Brightness temperature in K for the vertically polarized 22.2 GHz channel.
TB_F08_37H	Brightness temperature in K for the horizontally polarized 37.0 GHz channel.
TB_F08_37V	Brightness temperature in K for the vertically polarized 37.0 GHz channel.

Table 2. Field contents for Data Group "F08" for high frequency channels with 12.5 km resolution.

Parameter	Description
TB_F08_85H	Brightness temperature in K for the horizontally polarized 85.5 GHz channel.
TB_F08_85V	Brightness temperature in K for the vertically polarized 85.5 GHz channel.

Table 3. Field contents for Data Group “F17”for low frequency channels with 12.5 km resolution.

Parameter	Description
TB_F17_91H	Brightness temperature in K for the horizontally polarized 91.7 GHz channel.
TB_F17_91V	Brightness temperature in K for the vertically polarized 91.7 GHz channel

See Figure 1 and Figure 2 for sample brightness temperature browse images.

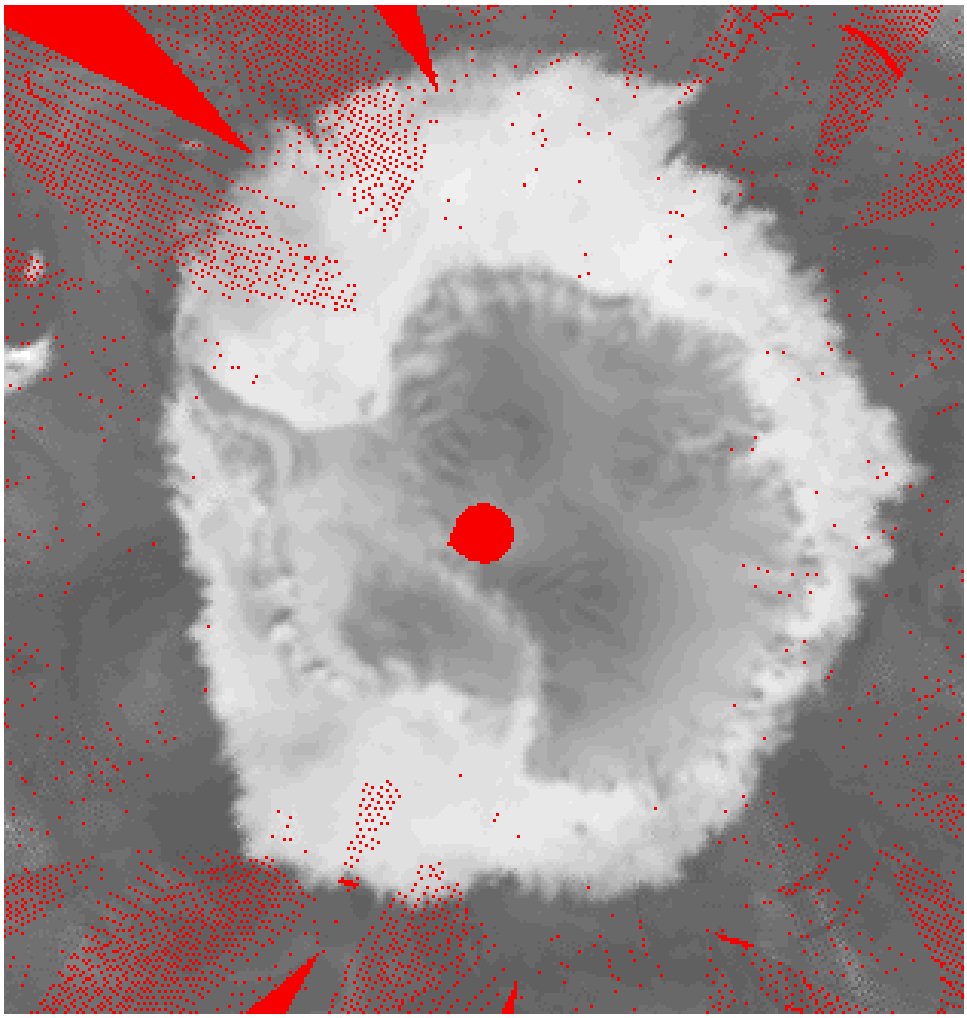

Figure 1. Sample brightness temperature image from the 19GHz-horizontally polarized channel of F08 on 10 October 1988 in Antarctica, where missing data are shown in red and brightness temperature data in grayscale.

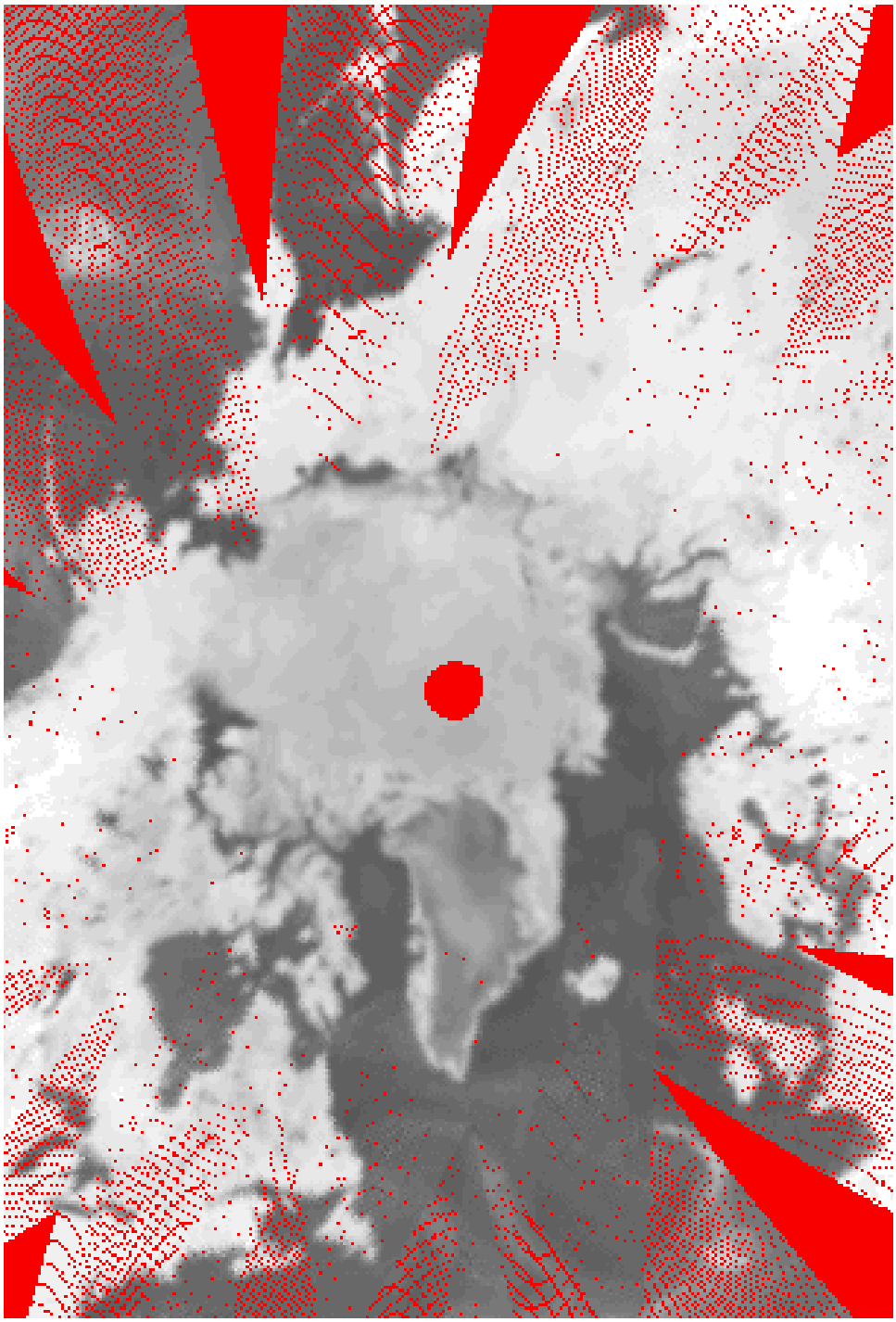

Figure 2. Sample brightness temperature image from the 19GHz-horizontally polarized channel of F08 on 10 October 1988 in the Arctic, where missing data are shown in red and brightness temperature data in grayscale.

1.2.3 Naming Convention

Files are named according to the following convention and as described in Table 4:

Generic File Name: NSIDC0001_TB_PS_HXkm_YYYYMMDD_vV.ext

Example File Name: NSIDC0001_TB_PS_N25km_20230103_v6.0.nc

Example File Name: NSIDC0001_TB_PS_S12.5km_20220523_v6.0.nc

Table 4. File Naming Convention Description

Variable	Description
TB	Identifies this as a file containing brightness temperatures
PS	Identifies the grid as Polar Stereographic spatial reference system
H	Hemisphere: Northern (N) or Southern (S)
Xkm	Grid cell size (example: 12.5 km or 25 km)
YYYY	4-digit year
MM	2-digit month
DD	2-digit day
vV	Data version number (example: v6)
.ext	File extension: NetCDF (.nc)

1.3 Spatial Information

1.3.1 Coverage

Instrument coverage is global except for directly over the poles. For the Special Sensor Microwave/Imager (SSM/I) sensor, locations poleward of 87.2° are never measured due to the orbital inclination of the satellites. For the Special Sensor Microwave Imager/Sounder (SSMIS) sensor, locations poleward of 89.2° are not measured.

1.3.2 Resolution

Gridded data resolution varies by frequency. The 19.3 GHz, 22.2 GHz, and 37.0 GHz data are provided at a resolution of 25 km, and the 85.5 GHz and 91.7 GHz data are mapped to a 12.5 km grid. However, because the polar grids are not equal area, the actual resolution varies by latitude.

1.3.3 Projection and Grid Description

The data are provided on the 25 km and 12.5 km Northern Hemisphere and Southern Hemisphere Polar Stereographic Grids, as described in Table 5 and Table 6. For more information, see the Polar Stereographic Projections web page.

Table 5. Geolocation Details by Projection (Hemisphere)

Geographic Coverage	Northern Hemisphere	Southern Hemisphere
Geographic coordinate system	Unspecified datum based upon the Hughes 1980 ellipsoid	Unspecified datum based upon the Hughes 1980 ellipsoid
Projected coordinate system	NSIDC Sea Ice Polar Stereographic North	NSIDC Sea Ice Polar Stereographic South
Longitude of true origin	-45	0
Latitude of true origin	70	-70
Scale factor at longitude of true origin	1	1
Datum	Not_specified_based_on_Hughes_1980_ellipsoid	Not_specified_based_on_Hughes_1980_ellipsoid
Ellipsoid/spheroid	Hughes 1980	Hughes 1980
Units	meter	meter
False easting	0	0
False northing	0	0
EPSG code	3411	3412
PROJ4 string	`+proj=stere +lat_0=90 +lat_ts=70 +lon_0=-45 +k=1 +x_0=0 +y_0=0 +a=6378273 +b=6356889.449 +units=m +no_defs`	`+proj=stere +lat_0=-90 +lat_ts=-70 +lon_0=0 +k=1 +x_0=0 +y_0=0 +a=6378273 +b=6356889.449 +units=m +no_defs`
Reference	https://epsg.io/3411	https://epsg.io/3412

Table 6. Grid Details by Grid Resolution

Nominal gridded resolution	12.5 km	25.0 km
Grid cell size (x, y)	12.5 km by 12.5 km	25.0 km by 25.0 km
Geolocated lower left point in grid	Northern Hemisphere: 33.92° N, 279.26° W Southern Hemisphere: 41.45° S, 225.00° W	
Number of rows	Northern Hemisphere: 896 Southern Hemisphere: 664	Northern Hemisphere: 448 Southern Hemisphere: 332
Number of columns	Northern Hemisphere: 608 Southern Hemisphere: 632	Northern Hemisphere: 304 Southern Hemisphere: 316

Grid rotation	N/A	N/A
ulxmap – x-axis map coordinate of the edge of the upper-left pixel (XLLCORNER for ASCII data)	Northern Hemisphere: -3850 projected km Southern Hemisphere: -3950 projected km	
ulymap – y-axis map coordinate of the edge of the upper-left pixel (YLLCORNER for ASCII data)	Northern Hemisphere: 5850 projected km Southern Hemisphere: 4350 projected km	

1.4 Temporal Information

1.4.1 Coverage

Data coverage began on 09 July 1987 and is ongoing through the most current processing. Table 7 lists the temporal coverage by satellite. See the "Acquisition" section of this document for dates by instrument and platform.

Table 7. Data Set Coverage by Platform

DMSP Platform	Sensor	Temporal Coverage
F8	SSM/I	1987-Jul-09 to 1991-Dec-31
F11	SSM/I	1991-Dec-03 to 1995-Sept-30
F13	SSM/I	1995-May-03 to 2007-Dec-31
F17	SSMIS	2006-Dec-14 to present
F18	SSMIS	2017-Jan-01 to present

1.4.2 Resolution

Data are daily averages of all Brightness Temperature (Tb) observations whose center point falls within each grid cell.

2 DATA ACQUISITION AND PROCESSING

2.1 Background

Passive microwave observations of polar oceans are used to identify the ice edge, estimate sea ice concentrations, and classify sea ice. These data can be useful for shipping and petroleum-development activities and for helping understand and model climate change.

2.2 Acquisition

Data are derived from the Special Sensor Microwave/Imager (SSM/I) sensor, mounted on the Defense Meteorological Satellite Program (DMSP) F8, F11, and F13 platforms, and the Special Sensor Microwave Imager/Sounder (SSMIS) sensor, mounted on DMSP F17 and F18 platforms. Table 6 shows the date ranges during which each sensor was used.

Brightness temperatures data are calculated at the following frequencies: 19.3, 22.2, 37.0, 85.5, and 91.7 GHz. Both horizontally (H) and vertically (V) polarized Tb are available for all frequencies, except for 22.2 GHz at which only vertically polarized Tb are available. Both the SSM/I and SSMIS sensors use the 19.3, 22.2, and 37.0 channels (channel is the combination of frequency and polarization, e.g., 19.3V). The SSM/I sensors use 85.5 high-frequency channels, while the SSMIS sensor uses the 91.7 high-frequency channels.

2.3 Processing

1. **NSIDC Receives Brightness Temperature Data from Remote Sensing Systems, Inc.**
   Raw satellite swath measurements are processed at Remote Sensing Systems, Inc. (RSS) in Santa Rosa, California. RSS then provides NSIDC with processed, geolocated, calibrated, and error-corrected Tb swath data. For more details about how the raw data are processed, please refer to the Remote Sensing Systems SSMI / SSMIS web page, the RSS calibration reports (Wentz 2010, Wentz 2013), and the RSS user manuals (Wentz 1988, Wentz 1991, and Wentz 1993).

2. **NSIDC Converts to Swath Format**
   The RSS Tb estimates are converted by NSIDC to a consistent swath format. The swath footprint size, or effective Field of View (FOV), varies by frequency and is described in Table 8.

Table 8. Effective Field of View (FOV) per Channel*

Channel Frequency	FOV
19.3 GHz	70 km x 45 km
22.2 GHz	60 km x 40 km
37.0 GHz	38 km x 30 km
85.5 GHz	16 km x 14 km
91.7 GHz	16 km x 13 km

* Channel is the combination of frequency and polarization, e.g., 19.3V or 91.7H.

3. **NSIDC Converts to the Polar Stereographic Grid**
   Data are gridded to either the 12.5 km or 25 km Polar Stereographic Projection using a simple sum-and-average method, also known as the drop-in-the-bucket method. Swath data are assigned to grid cells based on where the center of their footprint falls. Some grid cells are empty because no swath centers pass through them; these grid cells are given a value of zero to indicate that no data was available on that day. Daily Tb values represent the average of all swaths – usually between one and six swaths – that contribute to a grid cell each day.

2.4 Quality, Errors, and Limitations

Over the years, numerous corrections have been applied to the F8, F11, F13, F17, and F18 data. Users should use the most recent version of the data set, as well as the most recent tools, whenever working with this product.

2.4.1 Limitations

There are four main limitations to this data set.

1. Despite sea ice and land being the predominant surfaces covered in this data set, the RSS calibration methods are optimized for open ocean.
2. The various DMSP sensors experience different crossing times due to unique flight paths, and crossing times change over the course of each sensor's lifetime (see the web page about Crossing Times from Remote Sensing Systems for more details). These trajectory differences can change the location of swath footprints. As a result, grid cell values may differ between sensors, and comparisons between or across sensors are more difficult.
3. Whenever a new sensor is added (e.g. switching raw inputs from F11 to F13 measurements) or a new calibration method is initiated (e.g. switching from RSS V7 to RSS V8), earlier data are not reprocessed. When looking across the entire data record, users should pay special attention to these periods of change (as noted in Table 7). For a sense of how changes in sensor inputs and calibration methods affect the final data product, users should refer to the comparisons between sensors (Abdalati et al., 1995; Stroeve et al., 1997; Stroeve, 1998; Meier et al., 2011; Cavalieri et al., 2012).
4. Occasionally, observations may be assigned to the wrong grid cell because of geolocation uncertainty. The initial geolocation error was between 20 and 30 km (Poe and Conway, 1990), though further refinements reduced this error to approximately 8 km (Goodberlet, 1990).

For more details on known issues for specific sensors, please refer to the RSS Known Issues web page.

2.4.2 Differences Between F17 and F18 Data

NSIDC compared T_b data from the F17 and F18 sensors for the period between 01 January 2015 and 31 December 2015. On average, differences in T_b measurements between the sensors were less than 1 K (Stewart et al., 2019). The exception was the 22.2 GHz channel, which is sensitive to water vapor, so larger differences were expected. Difference standard deviations were typically less than 5 K (Stewart et al., 2019). A linear regression was also used to compare the two sensors. The results indicated slopes near 1, with y-intercepts also near 1, except for over water and for the 91.7 GHz frequency, which is likely due to atmospheric emissions (Stewart et al., 2019). Correlations between F17 and F18 were greater than 0.95 (Stewart et al., 2019).

The biggest differences between the F17 and F18 sensors were found in: (1) areas with steep T_b gradients, such as across land-ocean or land-ice boundaries, due to differences in sensor footprint patterns, and (2) regions of rapid change, such as the sea ice edge or under passing weather systems, due to differences in crossing times between the sensors. The smallest differences were due to internal calibration biases or effects of the daily composite gridding.

2.4.3 Differences Between F13 and F17 Data

NSIDC compared the F13 and F17 data for the period between 01 January 2007 and 31 December 2007. The vast majority of differences ranged between 0.5 K and 2 K. Some larger differences, up to 10 K, were found, primarily in regions with sharp gradients in brightness temperatures (e.g. along coasts and the ice edge). Smaller differences of 0.5 K to 2 K in some channels, such as 19.3V, 19.3H, 22.2V, and 37.0H, were likely due to the cross-sensor calibration. Users should refer to Meier et al. (2011) and Cavalieri et al. (2012) for more details.

2.4.4 Differences Between F11 and F13 Data

NSIDC compared the F11 and F13 data for the period between May and September 1995. Users should refer to Stroeve et al. (1997) for more details.

2.4.5 Differences between F8 and F11 Data

Abdalati et al. (1995) compared the F8 and F11 data over Antarctica and the Greenland Ice Sheet. Stroeve (1998) also compared the differences between the F8 and F11 data. Users should refer to either paper for more details.

2.4.6 Errors

On 5 April 2016, the solar panel on the F17 satellite shifted position, compromising the integrity of the 37.0 vertical polarization. On 25 May 2016, RSS implemented a fix, but the long-term quality of the data is still unknown. Users should be cautious when using these data.

The 85.5 GHz data from the DMSP F8 platform (1987 - 1991) are of considerably poor quality and users are cautioned against using these data. Please refer to Wentz (1991) for more details.

2.5 Instrumentation

2.5.1 Description

The instruments used to acquire this data set are the Special Sensor Microwave/Imager (SSM/I) sensor (Hollinger and Lo 1983, Hollinger et al., 1987, Hollinger 1989, Hollinger et al., 1990), mounted on the Defense Meteorological Satellite Program (DMSP) F8, F11, and F13 platforms, and the Special Sensor Microwave Imager/Sounder (SSMIS) sensor (Kunkee et al., 2008a, Kunkee et al., 2008b), mounted on F17 and F18 platforms. A brief description of each sensor is provided below. Users should refer to the SMMR, SSM/I, and SSMIS Sensors Summary for more details.

The SSM/I instrument is a seven-channel, four-frequency, orthogonally polarized, passive microwave radiometric system. The instrument measures combined atmosphere and surface radiances at 19.3 GHz, 22.2 GHz, 37.0 GHz, and 85.5 GHz frequencies. Horizontal and vertical polarization measurements are available at each frequency, with the exception of 22.2 GHz, for which only vertical polarization is available.

The SSMIS instrument is a conically-scanning passive microwave radiometer that harnesses the imaging capabilities of SSM/I (with coincident channels except that 91.7 GHz replaces 85.5 GHz) and the sounding capabilities of the DMSP SSM/T-1 temperature and SSM/T-2 water vapor sounders. The SSMIS sensor measures microwave energy at 24 frequencies between 19 and 183 GHz, with a swath width of 1700 km. This data set includes only the ground imaging channels that are consistent with the SSM/I channels.

3 SOFTWARE AND TOOLS

The data are provided in NetCDF format and can be read and viewed using software capable of interpreting this standard format. NASA's visualization software, Panoply (https://www.giss.nasa.gov/tools/panoply/), and the NetCDF Operator Toolkit (NCO found at http://nco.sourceforge.net/), suite of command line tools, have been used extensively at NSIDC to work with these data. A NSIDC GitHub repository (https://github.com/nsidc/polarstereo-reformat)

contains scripts that convert the NetCDF back to the original binary format from previous versions. For the lasted updated list of tools and the datasets that apply to them, see the Tools to Extract and Geolocate Polar Stereographic Data web page.

For more information regarding the latitude and longitude of the grids, see Polar Stereographic Ancillary Grid Information. For a comprehensive list of all polar stereographic tools and for more information, see the Polar Stereographic Data web page.

4 VERSION HISTORY

Table 9 outlines the processing and algorithm history for this product.

Table 9. Description of Processing Changes

Data Version	Sensor	Temporal Range	Source Data Version	Description of Changes
V6	F8, F11, F13, F17, and F18	09 Jul 1987 – (ongoing)	RSS V8	Version update reflects the conversion of the data set from binary to NetCDF. Daily files contain data from all available sensors for a particular day.
V5	F8, F11, F13, F17, and F18	09 Jul 1987 – (01 Jan 2021)	RSS V8	Version update reflects the beginning of the F18-derived data record. In addition, previous data files from the F8, F11, F13, and F17 sensors have been renamed to better conform to NSIDC storage system requirements. F8, F11, F13, and F17 data files were not reprocessed.
V4	F17	14 Dec 2006 – 31 Dec 2018	RSS V7	Version update reflects the beginning of the F17-derived data record. In addition to the new sensor, this version update coincides with RSS processing switching from V4 to V7. RSS V7 cross-calibrates between all SSM/I and SSMIS sensors, as well as AMSR-E and WindSat, improving consistency between all sensors.
V3	F13	01 July 2008 – 29 Apr 2009	RSS V6	Updated to include additional inter-sensor calibrations
V2	F13	03 May 1995 – 30 Jul 2008	RSS V4	Version update reflects the beginning of the F13-derived data record
V2	F11	03 Dec 1991 – 30 Sep 1995	RSS V3	N/A

V2	F8	09 Jul 1987 – 31 Dec 1991	RSS V3	N/A
V1	F8	Not available	N/A	Original version of data. Note: V01 was not indicated in Version 1 file names.

5 RELATED DATA SETS

- Bootstrap Sea Ice Concentrations from Nimbus-7 SMMR and DMSP SSM/I-SSMIS
- ESMR Polar Gridded Brightness Temperatures and Sea Ice Concentrations
- Near-Real-Time DMSP SSM/I-SSMIS Daily Polar Gridded Brightness Temperatures
- Near-Real-Time DMSP SSM/I-SSMIS Daily Polar Gridded Sea Ice Concentrations
- Nimbus-7 SMMR Polar Gridded Radiances and Sea Ice Concentrations
- DMSP SSM/I-SSMIS Pathfinder Daily EASE-Grid Brightness Temperatures
- Sea Ice Concentrations from Nimbus-7 SMMR and DMSP SSM/I-SSMIS Passive Microwave Data
- Sea Ice Trends and Climatologies from SMMR and SSM/I-SSMIS
- MEaSUREs Calibrated Enhanced-Resolution Passive Microwave Daily EASE-Grid 2.0 Brightness Temperature ESDR

6 ACKNOWLEDGMENTS

The authors are grateful to Roger Barry, Jim Maslanik, Julienne Stroeve, and Vince Troisi, who worked on previous versions of this data set.

7 REFERENCES

Abdalati, W., K. Steffen, C. Otto, and K. C. Jezek. 1995. Comparison of Brightness Temperatures from SSM/I Instruments on the DMSP F8 and F11 Satellites for Antarctica and the Greenland Ice Sheet. *International Journal of Remote Sensing* 16(7):1223-1229. https://dx.doi.org/10.1080/01431169508954473

Cavalieri, D. J., Parkinson, C. L., DiGirolamo, N., and A. Ivanoff. 2012. Intersensor calibration between F13 SSMI and F17 SSMIS for global sea ice data records. *IEEE Geoscience and Remote Sensing Letters* 9(2):233-236. https://dx.doi.org/10.1109/LGRS.2011.2166754.

Goodberlet, M. A. 1990. *Special Sensor Microwave/Imager Calibration/Validation.* Ph.D. dissertation submitted to the University of Massachusetts.

Hollinger, J. P. 1989. *DMSP Special Sensor Microwave/Imager Calibration/Validation.* Naval Research Labs: Washington, D.C. https://apps.dtic.mil/sti/citations/ADA274626

Hollinger, J. P. and R. C. Lo. 1983. *SSM/I Project Summary Report.* NRL Memorandum Report 5055. Naval Research Labs: Washington, D.C. https://apps.dtic.mil/sti/citations/ADA128803

Hollinger, J. P., R. C. Lo, R. Savage, and J. Pierce. 1987. *DMSP Special Sensor Microwave/Imager User's Guide.* Naval Research Labs: Washington, D.C.

Hollinger, J. P., J. L. Pierce, G. A. Poe. 1990. SSM/I Instrument Evaluation. *IEEE Transactions on Geoscience and Remote Sensing* 28(5):781-790. https://doi.org/10.1109/36.58964.

Kunkee, D. B., G. A. Poe, D. J. Boucher, S. D. Swadley, Y. Hong, J. E. Wessel, and E. A. Uliana. 2008a. Design and Evaluation of the First Special Sensor Microwave Imager/Sounder. *IEEE Transactions on Geoscience and Remote Sensing* 46(4):863-883. https://dx.doi.org/10.1109/TGRS.2008.917980.

Kunkee, D. B., S. D. Swadley, G. A. Poe, Y. Hong, and M. F. Werner. 2008b. Special Sensor Microwave Imager Sounder (SSMIS) Radiometric Calibration Anomalies-Part 1: Identification and Characterization. *IEEE Transactions on Geoscience and Remote Sensing* 46(4):1017-1033. https://dx.doi.org/10.1109/TGRS.2008.917213.

Meier, W. N., Khalsa, S. J. S., and M. H. Savoie. 2011. Intersensor calibration between F-13 SSM/I and F-17 SSMIs near-real-time sea ice estimates. *IEEE Trans. Geosci. Remote Sens.* 49:3343–3349. https://dx.doi.org/10.1109/TGRS.2011.2117433.

Poe, G. A. and R. W. Conway. 1990. A Study of the Geolocation Errors for the Special Sensor Microwave/Imager (SSM/I). *IEEE Transactions on Geoscience and Remote Sensing* 28(5):791-799. https://dx.doi.org/10.1109/36.58965.

Stewart, S., Wilcox, H., Meier, W., and D. Scott. 2019. Comparison of F17 and F18 Daily Polar Gridded SSMIS Data. The National Snow and Ice Data Center: Boulder, CO.

Stroeve, J., Li, X., and J. Maslanik. 1997. An Intercomparison of DMSP F11- and F13-derived Sea Ice Products. NSIDC Special Report-5. The National Snow and Ice Data Center: Boulder, CO.

Stroeve, J. 1998. Impact of Various Processing Options on SSM/I-derived Brightness Temperatures. NSIDC Special Report-7. The National Snow and Ice Data Center: Boulder, CO.

Wentz, F. J. 1988. User's Manual: SSM/I Antenna Temperature Tapes. Remote Sensing Systems, Inc., Santa Rosa CA. RSS Technical Report 032588.

Wentz, F. J. 1991. User's Manual: SSM/I Antenna Temperature Tapes. Rev. 1. Remote Sensing Systems, Inc., Santa Rosa, CA. RSS Technical Report 120191.

Wentz, F. J. 1993. User's Manual: SSM/I Antenna Temperature Tapes. Rev. 2. Remote Sensing Systems, Inc. Santa Rosa, CA. RSS Technical Report 120193.

Wentz, F. J. 2010. SSM/I Version-6 Calibration Report. Remote Sensing Systems, Inc., Santa Rosa CA. RSS Technical Report 102210.

Wentz, F. J. 2013. SSM/I Version-7 Calibration Report. Remote Sensing Systems, Inc., Santa Rosa CA. RSS Technical Report 011012.

8 DOCUMENT INFORMATION

8.1 Publication Date

November 2022

8.2 Date Last Updated

August 2023